Tetrahedron 69 (2013) 7102–7106

Contents lists available at SciVerse ScienceDirect

Tetrahedron

journal homepage: www.elsevier.com/locate/tet

A BODIPY-based sensor for Hg^{2+} in living cells

Taiping Zhang [a,b], Guangwei She [a], Xiaopeng Qi [a,b], Lixuan Mu [a,*]

[a] Key Laboratory of Photochemical Conversion and Optoelectronic Materials, Technical Institute of Physics and Chemistry, Chinese Academy of Sciences, Beijing 100190, China
[b] University of Chinese Academy of Sciences, Beijing 100049, China

ARTICLE INFO

Article history:
Received 4 March 2013
Received in revised form 5 June 2013
Accepted 8 June 2013
Available online 21 June 2013

Keywords:
Fluorescent probe
ICT
Mercury (II)
BODIPY

ABSTRACT

A BODIPY-based probe has been investigated for fast response to Hg^{2+} with high sensitivity and selectivity in living cells. This response is attributed to intramolecular charge transfer (ICT) mechanisms. The detection limit is lower than the upper limit (10 nM) that the United States Environmental Protection Agency (EPA) had mandated for Hg^{2+} in drinking water.

1. Introduction

Mercury ion (Hg^{2+}) is one of the most dangerous heavy metal ions.[1–5] Even at a low concentration, mercury ions can induce several human diseases, including acrodynia (pink disease), Hunter-Russell syndrome, and Minamata diseases, which result from the accumulation of mercury through biological chain.[6] Physiologically, mercury ions can also easily pass through biological membranes and cause serious damages to the central nerves and endocrine systems.[7,8] The upper limit of Hg^{2+} in drinking water is 10 nM as mandated by United States Environmental Protection Agency (EPA).[9] Thus, it is highly desirable to develop sensors for Hg^{2+}.

Fluorescence sensors have been widely developed to detect metal ions, organic molecules, and biological analytes. Such fluorescence sensors are superior because of their sensitivity, simplicity, and real-time analysis.[10,11] Especially, the fluorescence sensors are able to modulate the emission wavelength. In far red and near IR-emission region lights can transmit deeply into human body tissues without disturbing the normal physiological activities.[12] It is potential to be well adapted into many applications, such as in vivo biological imaging.[13,14]

BODIPY-based (Boradiazaindacenes, 4,4-Difluoro-4-bora-3a,4a-diaza-s-indacene) dyes are expected to be matrix of far red and near-IR dyes, because they possess desired characteristics, such as sharp absorption and fluorescence bands, high extinction coefficients, high fluorescence quantum yields, high stability against light, and easy modification[15–18] to exhibit fluorescence at wavelength beyond 650 nm by extending delocalization of the conjugated system. It is available to synthesize pyrrole derivatives bearing phenyl, vinyl, or thiophene groups at the 3-position to manipulate the characters and properties of this kind of BODIPY dyes.[19]

Knut Rurack et al. had developed BODIPY-based Hg^{2+} sensor by introducing the 1,4,7,10-tetrathia-13-az acyclopentadecane to the *meso* position of BODIPY,[20] however, the sensor emission was far from the far red or Near-IR region.[21] Yuliang Li et al. designed dithia-dioxa-aza macrocycles sensor of Hg^{2+} on the BODIPY chromophore,[1] but its detection limit did not meet the upper limit that the EPA had mandated for Hg^{2+} in drinking water. Our work aimed at the construction of Hg^{2+} sensor based on ICT (intramolecular charge transfer) mechanism The chromophore was designed to shift emission wavelengths to the far red region, i.e., the range beyond 650 nm. Furthermore, it was used for imaging in living cells with excellent performance.

To achieve goals mentioned above, Z1 (Scheme 1) was synthesized featuring a BODIPY fluorophore and a thia aza crown ether receptor (Scheme 1). (The thia aza crown ether receptor was reported to be selectively responsible for Hg^{2+}.[22])

* Corresponding author. Tel./fax: +86 10 82543513; e-mail address: mulixuan@mail.ipc.ac.cn (L. Mu).

0040-4020/$ – see front matter © 2013 Elsevier Ltd. All rights reserved.
http://dx.doi.org/10.1016/j.tet.2013.06.025

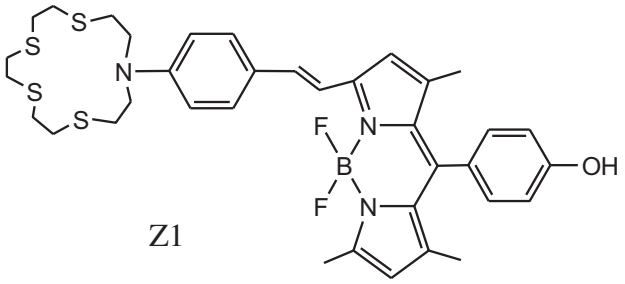

Scheme 1. The molecular structure of Sensor Z1.

2. Result and discussion

2.1. Physical characteristic of Z1

The photophysical properties of Z1 in different solvents were investigated, as shown in Table 1. From cyclohexane to acetonitrile, a significant bathochromic shift in the excitation (586–598 nm) and emission (609–656 nm) were observed along with the increased polarities of the solvents. The absorption maximum is located at 594 nm and has a hypsochromic shift of 12 nm from cyclohexane to acetonitrile–HEPES solution (Table 1), which is weak solvent dependence. In contrast, the fluorescence emission spectra are strongly dependent on the dipole moment of the solvents. The emission maximum shifts from 609 nm in cyclohexane to 656 nm in acetonitrile–HEPES solution.[23] The bathochromic shifts with a concomitant decrease of fluorescence quantum yield are observed (from 0.22 to 0.01). The reducing of the quantum yield is attributed to the acceleration of internal conversion; the bathochromic shift of the emission wavelength is due to the decreasing of the energy gap between the ground state and the excited state.[18] The data above confirmed that Z1 was going through ICT transformation.

Table 1
Absorption and emission properties of Z1 in different solvents

Solvent	λ_{abs} (max/nm)	λ_{em} (max/nm)	Φ_F
Cyclohexane	586	609	0.22
Toluene	596	618	0.15
Chloroform	598	621	0.10
Acetonitrile	591	648	0.02
Acetonitrile/HEPES=4/1	594	656	0.01

2.2. Computational results of Z1

According to the frontier orbital distribution in Fig. 1, the electron cloud density of the LUMO is considerably larger than that of the HOMO, which leads to an expected stabilization of the LUMO through irradiation.[17] The electron cloud density would be disturbed by external interferences. Hence, the energy gap between the HOMO and LUMO is expected to increase owing to the introduction of Hg^{2+} and the absorption has hypochromatic shift.[17] The band gap between LUMO and HOMO is 1.92 eV, which indicates the fluorescence emission of Z1 would be about 650 nm (far red region).

2.3. Spectral response of Z1 to Hg^{2+} and Ag^{+}

Fig. 2a shows the absorption spectral changes of Z1 as a function of the Hg^{2+} concentration in a CH_3CN–HEPES solution (4:1, *v*/*v*, pH=6.86) at room temperature. The UV–Vis spectrum of Z1 is characterized with an intense band centered at 594 nm, which is

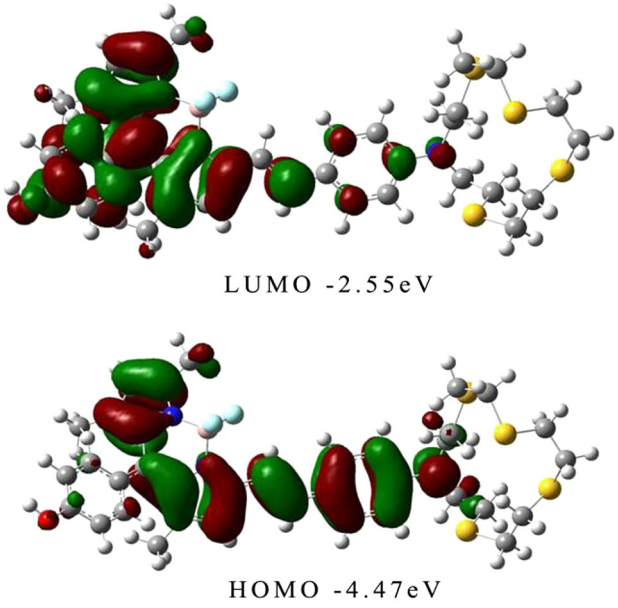

Fig. 1. HOMO (below) and LUMO (above) distributions of Z1.

responsible for the red color of the solution. The absorption maximum of Z1 has a bathochromic shift of about 90 nm in comparison with the standard BODIPY dye.[24] This red shift is assigned to an efficient ICT process from the donor nitrogen atom on the thia aza crown ether receptor that was conjugated to the BODIPY acceptor group.[23,25,26] Upon adding Hg^{2+}, the intensity of the absorption maximum of Z1 at 594 nm gradually decreased along with the formation of a new band centered at 564 nm, indicating that Hg^{2+} binded to thia aza crown ether. The coordination of Hg^{2+} to the ligand reduced the electron-donating ability of the nitrogen atom at the thia aza crown ether, thus the ICT effect decreased. Therefore, the blue-shift in absorption spectra was observed upon Hg^{2+} binding.

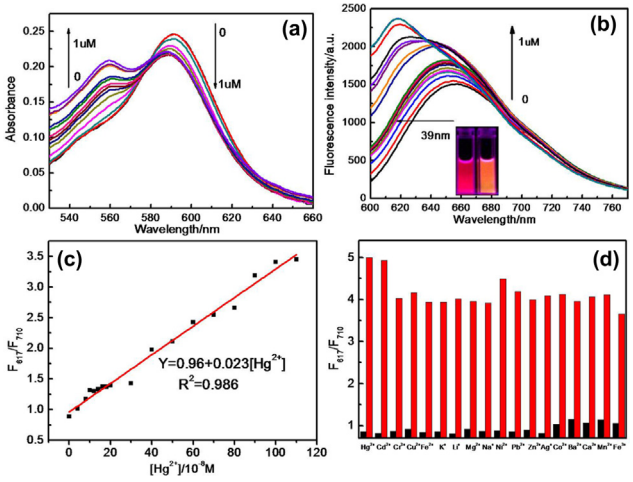

Fig. 2. (a) Absorption spectra of Z1 probe in CH_3CN and HEPES at pH 6.86 upon gradual addition of Hg^{2+} at concentrations of 0–1 μM. (b) Emission spectra of Z1 in the presence of increasing Hg^{2+} concentration (0–1 μM) in a CH_3CN–HEPES solution (*v*/*v*=4/1, pH=6.86). Excitation wavelength was 560 nm. The concentration of Z1 was 1 μM. Inset: the fluorescence color change of Z1 (left) and Z1-Hg^{2+} (right). (c): In emission spectra F_{617}/F_{710nm} as a function of Hg^{2+} concentration (0–1 μM). (d): black bars: In emission spectra F_{617}/F_{710nm} as a function of 50 equiv of Cd^{2+}, Cr^{3+}, Cu^{2+}, Fe^{2+}, K^{+}, Li^{+}, Mg^{2+}, Na^{+}, Ni^{2+}, Pb^{2+}, Co^{2+}, Ba^{2+}, Ca^{2+}, Mn^{2+}, Fe^{3+}, and Zn^{2+}, 5 equiv of Hg^{2+} and 10 equiv of Ag^{+} in CH_3CN–HEPES solution (*v*/*v*=4/1, pH=6.86). Red bar: to mix 5 equiv of Hg^{2+}.

The fluorescence spectra of Z1 upon addition of Hg^{2+} were displayed in Fig. 2b. Free Z1 showed a maximum fluorescence emission at 656 nm upon excitation at 560 nm in buffer solution (CH_3CN and HEPES (v/v=4:1, pH=6.86)). After binding with Hg^{2+}, Hg^{2+}-Z1 showed a large emission blue-shift of 39 nm, indicating that a disturbed ICT process. The fluorescence intensity gradually increased at 617 nm, and the ratio of emission intensities (F_{617}/F_{710}) varied from 0.8 to 3.5 (Fig. 2c, the ratio was used to eliminate the disturbance of Ag^+, and the explanation were listed below). This can be explained by utilizing the ICT process—Hg^{2+} would coordinate with the N atom of the thia aza crown ether, which might restrict the ICT process. With the increase of Hg^{2+} concentration, the fluorescence intensity of the solution increased and the color changed from red to orange under a UV light (Fig. 2b inset). According to titration experiments, Job's plot determined that Z1 and Hg^{2+} was 1/1 complexion (see Supplementary data). Probe Z1 can detect the Hg^{2+} concentration at 4.36×10^{-9} M (Limit of detection was calculated according to the method described by Demchemko.[27]), which is lower than the upper limit (10 nM) that the EPA had mandated for Hg^{2+} in drinking water.

To obtain an insight into the sensing properties of Z1 toward metal ions, the fluorescence emission of different ions in CH_3CN–HEPES solution (v/v=4:1, pH=6.86) was investigated, and the results were shown in Fig. 2d. No significant ratio (F_{617}/F_{710}) changes were observed when Cd^{2+}, Cr^{3+}, Cu^{2+}, Fe^{2+}, K^+, Li^+, Mg^{2+}, Na^+, Ni^{2+}, Pb^{2+}, Ag^+, Co^{2+} Ba^{2+} Ca^{2+} Mn^{2+} Fe^{3+}, and Zn^{2+} were added in the sensor solution even at high concentration (50 equiv, black bars). Completive experiments in the addition of Hg^{2+} (5 equiv) showed similar ratio (F_{617}/F_{710}) enhancement (Fig. 2d red bars). The result suggested that Z1 had good selectivity toward Hg^{2+}.

The emission spectrum changes of Z1 upon the addition of an increasing amount of Ag^+ were displayed in Fig. 3a. Free Z1 showed a maximum fluorescence emission at 656 nm upon excitation at 560 nm in buffer solution (CH_3CN–HEPES (v/v=4:1, pH=6.86)). Remarkable fluorescence enhancements were detected along the addition of Ag^+ while only a smaller wavelength shift (3 nm) appears. The disturbance of Ag^+ was eliminated by ratiometric signals.

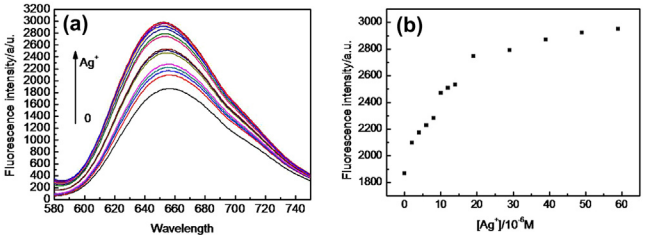

Fig. 3. (a) Emission spectra of Z1 along with the increased concentration of Ag^+ (0–10 equiv) in a CH_3CN–HEPES solution (v/v=4/1, pH=6.86). The excitation wavelength was 560 nm and the concentration of Z1 was 1 μM. (b) Fluorescence intensity of Z1 probe in CH_3CN and HEPES at pH 6.86 upon gradual addition of Ag^+ at concentrations of 0–10 equiv.

2.4. Mechanism of the sensing system

The dual titration of Ag^+ and Hg^{2+} was also conducted. Z1 in CH_3CN and HEPES was first titrated with 10 equiv Ag^+, and the fluorescence intensity was significantly enhanced without wavelength changes. Then 5 equiv Hg^{2+} was added, the wavelength had a hypochromatic shift about 39 nm (Fig. 4a). In a contrast experiment, 5 equiv Hg^{2+} was first added, and the fluorescence intensity enhanced with a blue-shift of 39 nm. Then 10 equiv Ag^+ was added, the fluorescence intensity decreased only a little without wavelength changes (Fig. 4b).

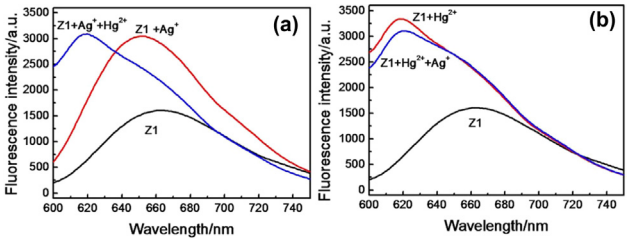

Fig. 4. (a) The fluorescence intensity changes of Z1: the curve (Z1+Ag^+) represents 10 equiv of Ag^+; the curve (Z1+Ag^++Hg^{2+}) represents 5 equiv of Hg^{2+} was added into the (Z1+Ag^+) solution. (b) The fluorescence intensity changes of Z1: the curve (Z1+Hg^{2+}) represents 5 equiv of Hg^{2+}; the curve (Z1+Hg^{2+}+Ag^+) represents 10 equiv of Ag^+ was added into the (Z1+Hg^{2+})solution. The concentration of Z1 was 1 μM.

Based on these data, we confirmed that Z1 had higher binding affinity for Hg^{2+} (3.19×10^6 M^{-1} obtained by nonlinear regression analysis, see Supplementary data) than that for Ag^+ (7.64×10^4 M^{-1} obtained by nonlinear regression analysis, see Supplementary data), which indicated the capacity that Hg^{2+} could displace Ag^+ to form more stable complexes and suggested the mechanism of sensing Ag^+ and Hg^{2+} (Fig. 5). Z1 can successfully distinguish Hg^{2+} from Ag^+ via two different sensing mechanisms, i.e., PET for Ag^+ and ICT&PET for Hg^{2+}. The reason might be that the Ag^+ does not get involved into the conjugated system while Hg^{2+} is involved, Ag^+ can only coordinate with four sulfur atoms of Z1 and result in fluorescence intensity enhancement. While, Hg^{2+} can coordinate with not only the four sulfur atoms but also the nitrogen atom and act as an electron-withdrawing group to regulate the electronic push–pull system, which consequently leads to fluorescence intensity enhancement and wavelength changes. Further investigation by leaving Z1 in a solution of pH=1 has showed that the emission wavelength hypochromatic shifts similar to Hg^{2+} (see Supplementary data). This is because H^+ can easily bind to the nitrogen atom but to the four sulfur atoms. This experiment also confirms the previous observation of the Ag^+ titration.

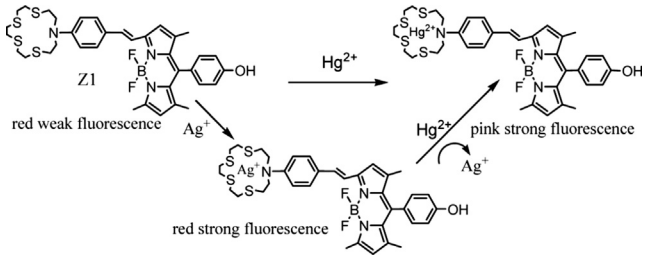

Fig. 5. The mechanism of Z1 for sensing Hg^{2+} and Ag^+.

2.5. Cell imaging

Live cell imaging based on Z1 was investigated with confocal laser scanning microscopy (CLSM). HeLa cells were utilized to demonstrate the utility of Z1 for intracellular Hg^{2+} sensing by cell imaging. After incubation with the Z1 solution (5 μM) for 15 min, the cells were washed three times in PBS buffer. The excitation wavelength was fixed at 561 nm. Fluorescent signals were collected from 600 nm to 650 nm. Fig. 6a–c shows cell images without the addition of Z1 in fluorescence image, bright field image, and overlay image, respectively. Fig. 6d–f shows the CLSM images of the Z1 stained HeLa cells in fluorescence image, bright field image, and overlay image, respectively. Weak fluorescence is observed in the cells. Fluorescence is hardly observed in the merged image. Fig. 6g–i shows the increases of the fluorescence intensity in living cells after addition of Hg^{2+} (50 μM) into the medium and incubated

for 10 min in fluorescence image, bright field image, and overlay image, respectively. Strong fluorescence is observed from the cellular cytoplasm in both the fluorescence image and overlayed image for the HeLa cells. The results reveal that Z1 can penetrate the living cell membrane and be used for imaging intracellular Hg^{2+} in living cells.

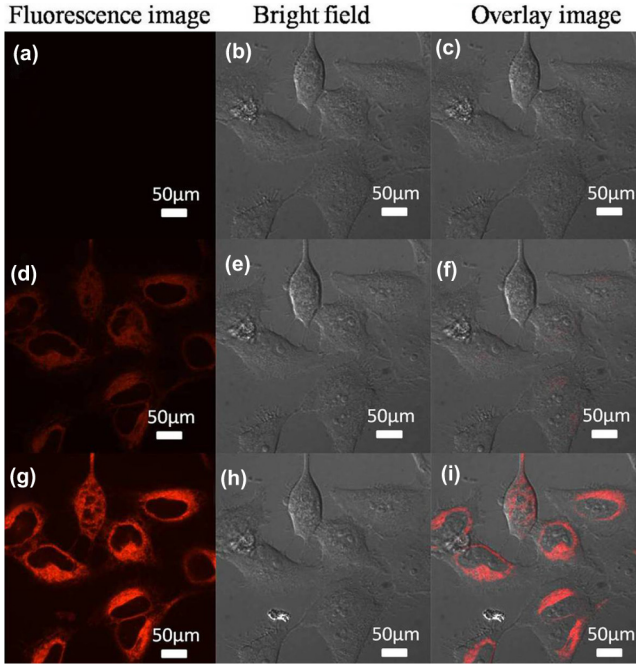

Fig. 6. Confocal fluorescence images of living HeLa cells. (a), (b), (c) Blank. (d), (e), (f) Incubated with Z1 (5 μM) for 15 min. (g), (h), (i) Then further incubated with 50 μM Hg $(ClO_4)_2$ for 10 min.

3. Conclusions

We have developed a BODIPY-based ICT sensor with far red emission for Hg^{2+} detection. The sensor exhibits high sensitivity with a detection limit of 4.36 nM and high selectivity over other metal ions including Cd^{2+}, Cr^{3+}, Cu^{2+}, Fe^{2+}, K^{+}, Li^{+}, Mg^{2+}, Na^{+}, Ni^{2+}, Pb^{2+}, Co^{2+} Ba^{2+} Ca^{2+} Mn^{2+} Fe^{3+}, and Zn^{2+}. This work also provides a basis for further investigation of BODIPY-based sensors and improves the characteristics of BODIPY.

4. Experiment section

4.1. Materials and apparatus

All UV—Vis and fluorescence spectra in this work were recorded with Hitachi U3010 spectrometers and Hitachi F-4600 fluorescence spectrometers, respectively. The quantum yield of Z1 in different solvents was directly obtained through the FLS920 Combined Steady State & Time Resolved Fluorescence Spectrometer. ^{1}H NMR (400 Hz) and ^{13}C NMR (100 Hz) spectra were obtained on a Bruker Avance 400 NMR spectrometer using tetramethylsilane (TMS) as an internal reference.

Unless otherwise noted, all reagents were purchased from commercial suppliers and were used without further purifications.

4.2. Synthesis (Scheme 2)

1,4,8,11-Tetrathiaundecane (Z5) was synthesized according to the literature.[28]

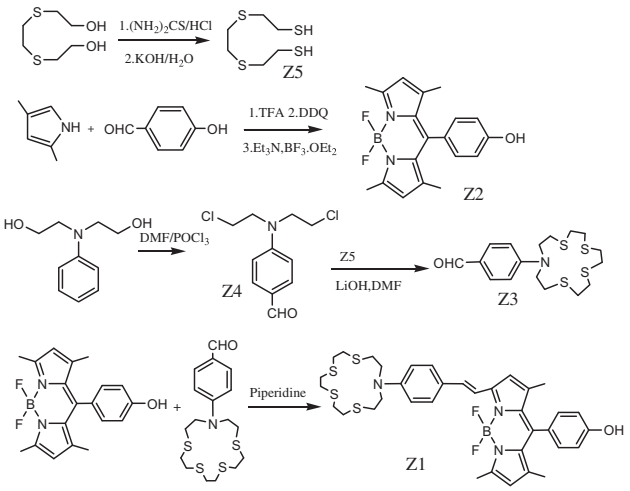

Scheme 2. The synthesis of sensor Z1.

4,4-difluoro-8-(4′-hydroxyphenyl)-1,3,5,7-tetramethyl-4-bora-3a,4a-diaza-s-indacene (Z2) was synthesized according to the literature.[29]

4.2.1. Synthesis of 4-(bis(2-chloroethyl)amino)benzaldehyde (Z4). 1.81 g (10 mmol) *N*,*N*-diethoxy aniline, 5 mL $POCl_3$, and 10 mL DMF were mixed and the thus-formed solution was refluxed for 5 h. The reaction mixture was poured into ice water, extracted with dichloromethane (3×100 mL). The organic layers were combined and dried over magnesium sulfate, and then the solvent was removed under reduced pressure. The residue was purified by column chromatography through silica gel with ethyl acetate and petroleum ether (*v*:*v*=1:5) as eluent to afford a yellow solid, which was further recrystallized from ethyl acetate and petroleum ether (*v*:*v*=1:5) to yield 0.85 g (35%) yellow crystal. ^{1}H NMR ($CDCl_3$): δ=3.68 (t, 4H), δ=3.83 (t, 4H), δ=6.74 (s, 2H), δ=7.78 (s, 2H), δ=9.79 (s, 1H). $C_{11}H_{13}Cl_2NO$ calcd for 245.04 found 245.091.

4.2.2. Synthesis of 13-(4-formylphenyl)-1,4,7,10-tetrathia-13-az acyclopentadecane (Z3). 735 mg (3 mmol) Z2, 642 mg (2.6 mmol) Z4, and 360 mg (15 mmol, 5 equiv) LiOH were mixed in 100 mL DMF, and the thus-formed solution was refluxed for 10 h. The solvent was removed under reduced pressure and the resultant residue was purified by column chromatography over silica gel with dichloromethane and methanol (*v*:*v*=3:1) as eluent to afford a pale yellow liquid (0.38 g, 30%). ^{1}H NMR ($CDCl_3$): δ=2.75 (m, 10H), δ=3.40 (m, 6H), δ=3.68 (t, 2H), δ=3.85 (t, 2H), δ=6.92 (s, 2H), δ=7.74 (s, 1H), δ=9.90 (s, 1H). $C_{17}H_{25}NOS_4$ calcd for 387.08 found 387.084.

4.2.3. Synthesis of 3-{[13-(4-formylphenyl)-1,4,7,10-tetrathia-13-az acyclopentadecane]ethenyl}-4,4-difluoro-8-(4′-hydroxyphenyl)-1,3,5,7-tetramethyl-4-bora-3a,4a-diaza-s-indacene (Z1). 387 mg Z3 (1 mmol), 340 mg Z2 (1 mmol), and one drop of piperidine were refluxed in toluene under nitrogen for 10 h. Then the solvent was removed under reduced pressure.[19] The residue was purified by column chromatography over silica gel with dichloromethane and ethyl acetate (*v*:*v*=2:1) to afford a green solid (70 mg, 10%). ^{1}H NMR ($CDCl_3$): δ=1.54 (m, 6H), δ=1.57 (m, 3H), δ=2.64 (m, 1H), δ=2.74 (s, 3H), δ=2.77 (s, 3H), δ=7.58 (m, 6H), δ=2.93 (d, 3H), δ=3.26 (m, 6H), δ=3.28 (m, 6H), δ=3.36 (m, 8H), δ=6.89 (t, 3H), δ=7.76 (m, 6H), δ=7.99 (d, 2H), δ=9.79 (s, 1H), ^{13}C NMR ($CDCl_3$): δ (ppm) 24.8, 25.1, 26.6, 31.5, 36.5, 40.7, 46.9, 48.6, 114.7, 117.0, 128.5, 131.8, 154.5, 160.9, 162.6, 190.4. $C_{36}H_{42}BF_2N_3OS_4$ calcd for 709.23 found 709.346.

4.3. Computational methods

Orbital energies were calculated by using Gaussian 03 at B3LYP density functional theory (DFT). The calculation was carried out with the Gaussian 03 program package.[30]

4.4. General procedures for metal ion detection

Z1 (1 mM) was prepared by dissolving Z1 in CH_3CN–HEPES solution (v/v=4/1, pH=6.86), which was then diluted with CH_3CN–HEPES solution (v/v=4/1, pH=6.86) to prepare the solution of Z1 (10^{-6} mol L^{-1}). Solutions of other various ions were prepared by dissolving their perchloride salts in water. All measurements were operated according to the following procedure: 2 mL Z1 (10^{-6} mol L^{-1}) solution was filled in fluorescent cell, and then the ions were titrated with transferpette.

4.5. General procedures for cell incubate

HeLa cells (gifted from the center of cells, Peking Union Medical College) were cultured in confocal dishes in culture media (DMEM supplemented with 10% PBS, 50 unit/mL penicillin, and 50 mg/mL of streptomycin) and under 5% carbon dioxide/air at 37 °C in a humidified incubator. After 24 h, the cells were incubated with Z1 for 15 min. The cells were washed with PBS five times, and their fluorescence images were recorded by confocal fluorescence microscopy.

Acknowledgements

This work was financially supported by the Chinese Academy of Sciences, NSFC (grant nos. 51272302, 50902134, 21103211).

Supplementary data

Supplementary data related to this article can be found at http://dx.doi.org/10.1016/j.tet.2013.06.025.

References and notes

1. Yuan, M.; Li, Y.; Li, J.; Li, C.; Liu, X.; Lv, J.; Xu, J.; Liu, H.; Wang, S.; Zhu, D. *Org. Lett.* **2007**, *9*, 2313–2316.
2. Zhu, M.; Yuan, M.; Liu, X.; Xu, J.; Lv, J.; Huang, C.; Liu, H.; Li, Y.; Wang, S.; Zhu, D. *Org. Lett.* **2008**, *10*, 1481–1484.
3. Atilgan, S.; Ilker, K.; Tugba, O. *Tetrahedron Lett.* **2010**, *51*, 892–894.
4. Vedamalai, M.; Wu, S. P. *Org. Biomol. Chem.* **2012**, *10*, 5410–5416.
5. Vedamalai, M.; Wu, A. S. *Eur. J. Org. Chem.* **2012**, 1158–1163.
6. Grandjean, P.; Weihe, P.; White, R. F.; Debes, F. *Environ. Res.* **1998**, *77*, 165–172.
7. Zhang, X.; Xiao, Y.; Qian, X. *Angew. Chem., Int. Ed.* **2008**, *47*, 8025–8029.
8. Gutknecht, J. *J. Membr. Biol.* **1981**, *61*, 61–66.
9. Nolan, E. M.; Lippard, S. J. *Chem. Rev.* **2008**, *108*, 3443–3480.
10. Zhang, J.; Campbell, R. E.; Ting, A. Y.; Tisen, R. Y. *Nat. Rev. Mol. Cell Biol.* **2002**, *3*, 906–918.
11. de Silva, A. P.; Eilers, J.; Zlokarnik, G. *Proc. Natl. Acad. Sci. U.S.A.* **1999**, *96*, 8336–8337.
12. Weissleder, R. *Nat. Biotechnol.* **2001**, *19*, 316–317.
13. Medintz, I. L.; Uyeda, H. T.; Goldman, E. R.; Mattoussi, H. *Nat. Mater.* **2005**, *4*, 435–446.
14. Hinds, S.; Myrskog, S.; Levina, L.; Koleilat, G.; Yang, J.; Kelley, S. O.; Sargent, E. H. *J. Am. Chem. Soc.* **2007**, *129*, 7218–7219.
15. Murale, D. P.; Lee, K. M.; Kim, K.; Churchill, D. G. *Chem. Commun. (Camb.)* **2011**, 12512–12514.
16. Chen, J.; Burghart, A.; Derecskei-Kovacs, A.; Burgess, K. *J. Org. Chem.* **2000**, *65*, 2900–2906.
17. Lu, H.; Zhang, S.; Liu, H.; Wang, Y.; Shen, Z.; Liu, C.; You, X. *J. Phys. Chem. A* **2009**, *113*, 14081–14086.
18. Loudet, A.; Burgess, K. *Chem. Rev.* **2007**, *107*, 4891–4932.
19. Ulrich, G.; Ziessel, R.; Harriman, A. *Angew. Chem. Int. Ed.* **2008**, *47*, 1184–1201.
20. Rurack, K.; Kollmannsberger, M.; Resch-Genger, U.; Daub, J. *J. Am. Chem. Soc.* **2000**, *122*, 968–969.
21. Wang, H.; Wu, S. *Tetrahedron* **2013**, *69*, 1965–1969.
22. Ishikawa, J.; Sakamoto, H.; Wada, H. *J. Chem. Soc., Perkin Trans. 1* **1999**, 1273–1280.
23. de Silva, A. P.; Gunaratne, H. Q.; Gunnlaugsson, T.; Huxley, A. J.; McCoy, C. P.; Rademacher, J. T.; Rice, T. E. *Chem. Rev.* **1997**, *97*, 1515–1566.
24. Kollmannsberger, M.; Rurack, K.; Resch-Genger, U.; Daub, J. *J. Phys. Chem. A* **1998**, *102*, 10211–10220.
25. Rurack, K.; Kollmannsberger, M.; Daub, J. *Angew. Chem. Int. Ed.* **2001**, *40*, 385–387.
26. Coskun, A.; Akkaya, E. U. *J. Am. Chem. Soc.* **2005**, *127*, 10464–10465.
27. Demchemko, A. P. *Introduction to Fluorescent Sensing*; Springer: Ukraine38–39.
28. Yoon, S.; Albers, A. E.; Wong, A. P.; Chang, C. J. *J. Am. Chem. Soc.* **2005**, *127*, 16030–16031.
29. Coskun, A.; Deniz, E.; Akkaya, E. U. *Org. Lett.* **2005**, *7*, 5187–5189.
30. Frisch, M. J; Trucks, G. W.; Schlegel, H. B.; Scuseria, G. E.; Robb, M. A.; Cheeseman, J. R., Jr; Montgomery, J. A.; Vreven,, T.; Kudin, K. N.; Burant, J. C.; Millam, J. M.; Iyengar, S. S.; Tomasi, J.; Barone, V.; Mennucci, B.; Cossi, M.; Scalmani, G.; Rega, N.; Petersson, G. A.; Nakatsuji, H.; Hada, M.; Ehara, M.; Toyota, K.; Fukuda, R.; Hasegawa, J.; Ishida, M.; Nakajima, T.; Honda, Y.; Kitao, O.; Nakai, H.; Klene, M.; Li, X.; Knox,, J. E.; Hratchian, H. P.; Cross, J. B.; Bakken, V.; Adamo, C.; Jaramillo, J.; Gomperts, R.; Stratmann, R. E.; Yazyev, O.; Austin, A. J.; Cammi, R.; Pomelli, C.; Ochterski, J. W.; Ayala, P. Y.; Morokuma, K.; Voth, G. A.; Salvador, P.; Dannenberg, J. J.; Zakrzewski, V. G.; Dapprich, S.; Daniels, A. D.; Strain, M. C.; Farkas, O.; Malick, D. K.; Rabuck, A. D.; Raghavachari, K.; Foresman, J. B.; Ortiz, J. V.; Cui, Q.; Baboul, A. G.; Clifford, S.; Cioslowski, J.; Stefanov, B. B.; Liu, G.; Liashenko, A.; Piskorz, P.; Komaromi, I.; Martin, R. L.; Fox, D. J.; Keith, T.; Al-Laham, M. A.; Peng,, C. Y.; Nanayakkara, A.; Challacombe, M.; Gill, P. M. W.; Johnson, B.; Chen, W.; Wong, M. W.; Gonzalez, C.; Pople, J. A.; Gaussian: Wallingford CT.